Bone Reports 25 (2025) 101844

Contents lists available at ScienceDirect

Bone Reports

journal homepage: www.elsevier.com/locate/bonr

# Bone mechanical loading reduces heart rate and increases heart rate variability in mice

Julian A. Vallejo [a,b], Mark Gray [a], Jackson Klump [a], Andrew Wacker [a], Mark Dallas [b], Mark L. Johnson [b], Michael J. Wacker [a,*]

[a] University of Missouri – Kansas City, School of Medicine, Department of Biomedical Sciences, USA
[b] University of Missouri – Kansas City, School of Dentistry, Department of Oral & Craniofacial Sciences, USA

ARTICLE INFO

*Keywords:*
Bone compressive loading
Electrocardiogram
Parasympathetic nervous system
Sympathetic nervous system
Autonomic tone
Aging
Bone-heart crosstalk

ABSTRACT

Cardiovascular disease and osteoporosis are clinically associated. Bone adapts to mechanical forces by altering its overall structure and mass. In response to mechanical strain bone cells release signaling molecules and activate the nervous system. Bone also exhibits endocrine functions that modulate a number of tissues including the heart. We hypothesized that bone mechanical loading acutely alters cardiac function via neural and/or endocrine mechanisms. To test this hypothesis, we performed in vivo tibia mechanical loading in anesthetized mice while monitoring heart parameters using electrocardiogram (ECG). An immediate, transient reduction in resting heart rate was observed during tibial loading in both adult male and female mice ($p < 0.01$) with concurrent increases in heart rate variability (HRV) ($p < 0.01$). ECG intervals, PR, QRS and QTc were unaffected with loading. In further studies, we found that at least 3 N of load was necessary to elicit this heart response in adult mice. With aging to 11–12 months the responsiveness of the heart to loading was blunted, suggesting this bone-heart connection may weaken with age. Administration of lidocaine around the tibia significantly diminished the heart rate response to bone loading ($p < 0.05$). Moreover, pre-treatment with sympathetic antagonist propranolol inhibited this heart rate response to loading ($p < 0.05$), while parasympathetic antagonist atropine did not ($p > 0.05$). This suggests that a neuronal afferent pathway in the hindlimb and reduction in efferent sympathetic tone mediate this bone-neuro-heart reflex. In conclusion, the findings that tibia bone loading age-dependently modulates heart function support the concept of physiological coupling of the skeletal and cardiovascular systems.

## 1. Introduction

Bone provides both structural and regulatory roles including serving as a master regulator of serum phosphate via the actions of the bone-secreted hormone, fibroblast growth factor 23 (FGF23) in the kidney (Bonewald and Wacker, 2013), the dysregulation of which can lead to cardiovascular disease (Touchberry et al., 2013; Graves et al., 2021). Apart from FGF23 signaling, bone may also have additional influences in maintaining cardiac homeostasis. Deterioration of bone structure, mass and anabolic capacity, as experienced with osteoporosis, is strongly clinically associated with the development of cardiovascular dysfunction, even when controlling for traditional risk factors (Rodríguez-Gómez et al., 2022; Marcovitz et al., 2005; Tankó et al., 2005). This suggests a common etiology of these conditions. Autonomic dysfunction has been previously documented in those with compromised bone as a study measuring the frequency domain parameters of HRV in osteoporosis patients revealed significant alterations, indicating lower parasympathetic and higher sympathetic tone compared to those with normal bone mass (Tosun et al., 2011). In addition, a retrospective study among the 2009–10 Korea National Health and Nutritional Examination Survey in hypertensive individuals found an inverse association between resting heart rate and bone mineral density (Jung et al., 2018). Furthermore, beta blockers show dual efficacy in treating cardiovascular dysfunction and improving bone quality (Lary et al., 2020). The role of autonomic dysfunction in cardiovascular disease is of great clinical significance (Fang et al., 2020; Böhm et al., 2015), and cardiovascular disease remains the major cause of mortality and disability worldwide notwithstanding the progress made in cardiovascular disease treatment and prevention measures (Bansilal et al., 2015).

The skeleton is highly sensitive to mechanical stimuli from the

* Corresponding author at: 2411 Holmes, Kansas City, MO 64108, USA.
*E-mail address:* wackerm@umkc.edu (M.J. Wacker).

https://doi.org/10.1016/j.bonr.2025.101844
Received 1 April 2025; Accepted 14 April 2025
Available online 16 April 2025

environment, adapting its overall structure and mass accordingly in order to meet the demands of daily physical strains. Osteocytes, the most abundant cell type in bone tissue (>90 %), and osteoblasts, the precursors to osteocytes, both play pivotal roles in the sensation of mechanical strain and transduction of this signal into a bone formation/remodeling response, termed mechanotransduction (Tatsumi et al., 2007; Norvell et al., 2004; Tomlinson et al., 2017). Osteocytes reside inside the mineralized bone environment within fluid filled cavities known as lacunae and are connected with other osteocytes by numerous dendritic processes through a network of canals called the lacunocanalicular system (Robling and Bonewald, 2020). This osteocyte network allows for integrated cell-to-cell communication and connections to the vasculature, making it a suitable platform for sensation of mechanical strains (Kola et al., 2020). Osteoblasts, on the other hand, localize to the periosteal and endosteal bone surfaces, where they function in de novo bone formation. Mechanical loading induces deformations in the bone microenvironment as well as alterations to interstitial fluid flow pressure and shear stress around resident bone cell bodies (Bonewald and Johnson, 2008). Both osteoblasts and osteocytes respond to fluid flow stimulus through the rapid release of signaling molecules including, nitric oxide, ATP, and prostaglandin $E_2$ ($PGE_2$) (Dallas et al., 2013; Kamel et al., 2010). Downstream targets of these early response elements to loading include activation of the Wnt/β-catenin signaling pathway which further facilitates bone anabolic changes (Kamel et al., 2010; Robinson et al., 2006). In addition, osteocytes synthesize and release the negative regulators of bone mass including Wnt receptor antagonist, sclerostin (Li et al., 2005), and RANKL, which activates osteoclast differentiation and bone resorption in a paracrine manner (Nakashima et al., 2011).

Recent studies primarily from mouse models have elucidated an intimate relationship among bone and the central and peripheral nervous systems in mechanotransduction and regulation of bone mass. Bone development/repair and nerve growth in bone are tightly coupled (Li et al., 2019). Recently, sensory nerve fibers within bone have been shown to be a necessary component for the response to mechanical load, owing to binding of secreted PGE2 and neural growth factor from osteoblasts/osteocytes and relay of this afferent signal to the ventromedial hypothalamus (Tomlinson et al., 2017; Chen et al., 2019). Neural components of the autonomic nervous system, including the sympathetic nervous system (SNS) are also abundantly localized within bone tissue (Sayilekshmy et al., 2019) and, at least in rodents, play a pivotal role in neural efferent control of bone mass in response to mechanical loading (Chen et al., 2019; Gao et al., 2024). In addition to relaying osteogenic cues, the autonomic nervous system innervates and modulates functional output of nearly all major organ systems in the body including fat, liver, kidney, intestines, lungs, blood vessels, and heart (Elefteriou, 2018). The nearly ubiquitous distribution of the autonomic nerves throughout the body ensures extensive connections among organ systems to maintain homeostatic balance. Therefore, it is possible that bone-derived factors that trigger sensory neural afferents and activate the autonomic nervous system may also affect other organs such as the heart.

Bone also displays endocrine functions believed to be important for the homeostasis of many organ systems, implicating bone-derived hormones as potential central regulators of systemic health (Karsenty and Olson, 2016). PGE2 is released during bone mechanical loading from osteocytes in large quantities, likely through CX43 hemichannels, into the surrounding bone matrix and can affect osteoblasts and osteoclasts at the bone surface (Cherian et al., 2005). Our group has reported that the actions of bone-secreted factors may also extend beyond bone and impact skeletal muscle physiology, suggesting a para/endocrine pathway between bone and skeletal muscle. Administration of PGE2 to skeletal muscle myoblasts enhanced proliferation and fusion into differentiated myofibers (Mo et al., 2015; Mo et al., 2012). Moreover, conditioned media from bone cells increased myofiber calcium release and whole muscle contractile force output in mice (Mo et al., 2012; Huang et al., 2017). Another hormone released by bone into the circulation, undercarboxylated osteocalcin, has shown beneficial modulatory effects on a variety of tissues and is a potential treatment for metabolic disease (Ferron et al., 2012). Recently, undercarboxylated osteocalcin levels were reported to be upregulated in the serum of humans and rodents immediately after running exercise (Mera et al., 2016) and, at least in mice, appears to regulate heart rate during periods of acute stress via the autonomic nervous system (Berger et al., 2019).

The clinical associations among bone and heart health and the accumulating physiological evidence of bone as a regulator of other organs such as the heart, suggest potential crosstalk among bone mechanical loading and the heart. The physiological impact of bone mechanical loading in isolation from other systemic interactions on cardiac function in vivo is presently not well understood. We hypothesized that mechanical loading in bone would result in altered cardiac function in mice in vivo via neural and/or endocrine mechanisms. In the current study, we tested this hypothesis using compressive mechanical loading in the tibia of anesthetized mice and analyzed ECG parameters to determine effects on cardiac function. We also performed bone loading in the presence of various inhibitors to determine if the effects of bone loading on the acute heart rate changes are due to a neural or endocrine pathway.

## 2. Materials & methods

### 2.1. Animals

All animal procedures were approved by the University of Missouri-Kansas City Institutional Animal Care and Use Committee (UMKC-IACUC). Male and Female CD-1 background TOPGAL mice (β-catenin reporter mouse which carries a lacZ gene under the control of the TCF/Lef promoter) (#004623, Jackson Labs) (Lara-Castillo et al., 2015) aged to 5–6 months, and wild type CD-1 male mice ages 2–6 months (adult) and 11–12 months (middle age) (Envigo, Indianapolis, IN) were utilized for all mechanical loading studies. Mice were group-housed in a temperature controlled facility with a 12 h light-dark cycle and ad libitum access to food (#2918, Teklad Global, Madison, WI) and water. Animals were randomly assigned to different study groups and investigators were not blinded to these identities. All mice were sacrificed by cervical dislocation at the end of each experiment.

### 2.2. Tibia axial mechanical loading

Mice were maintained on isoflurane anesthesia (3 %, 1.5 L/min) via a Fortec vaporizer and secured in a precision bone loading apparatus (Bose, Electroforce 3220, MA, USA). Tibia compressive loading was performed as we have previously described (Robinson et al., 2006) with some modifications. Briefly, the right hindlimb of the mouse was positioned for axial loading of the tibia with the heel of the paw secured and the knee in contact with the loading cell. A pre-load of 0.5 N was applied to the loading cell to maintain the hindlimb in position prior to implementation of the loading protocol. For the acute loading protocol in 5–6 month old TOPGAL mice, the tibia was cyclically loaded with 9 N of force at a frequency of 2 Hz for 300 cycles lasting two and a half minutes ($n = 7$ male control, n = 7 male loaded; $n = 6$ female control, n = 7 female loaded). Loading at 9 N was chosen as it generates sufficient strain to induce a bone anabolic response in the tibia. The acute loading protocol (2 Hz, 300 cycles lasting 2.5 min) was also performed in 2–6 month old CD-1 male mice with 0 N (control $n = 15$), 1 N ($n = 8$), 2 N (n = 8), 3 N ($n = 12$) or 9 N ($n = 13$) of force. For these experiments, mice received loading at two randomized loading magnitudes with the lowest load applied first in the series and the highest load applied last. Additionally, the acute loading protocol (2 Hz, 300 cycles lasting 2.5 min) was performed in 11–12 month old CD-1 male mice with a force of 3 N followed by 9 N after a 10 min rest period in the same animal ($n = 13$ per group). Of these 11–12 month old mice, a subset was monitored for an

additional 15 min after the loading session ($n = 10$ per group). The concentration of isoflurane was maintained at 3 % for consistency with experiments using young adult mice, but the aged animals did not survive as well as the young animals and two control mice and four loaded mice died from complications related to anesthesia before completing the experiment. For all experiments, control mice were anesthetized and right hindlimb secured in the loading apparatus under 0.5 N preload for the same amount of time as loaded mice but did not receive the dynamic compressive loading.

### 2.3. In vivo electrocardiogram (ECG)

ECG was recorded during the loading experiments in anesthetized mice using 29-guage needle electrodes (ADInstruments) inserted subcutaneously in each of the limbs to obtain a six-lead ECG. Body temperature was maintained at physiological temperature using a water-jacketed heating pad and monitored via a rectal probe. ECG signals and body temperature were recorded using a PowerLab system with LabChart 8 software (ADInstruments). An ECG baseline was established for 5–8 min prior to loading, during the loading process, and during a 15-minute period subsequent to loading. Analysis of heart rate was performed by averaging over an interval of five seconds of data collection during baseline just before loading, during loading at the lowest heart rate, and at specific time intervals after the loading procedure. Heart rate variability (HRV) and lead II ECG signal intervals were analyzed by averaging over an interval 30 s of data collection during baseline just before loading, during loading at the lowest heart rate, and at specific time intervals after the loading procedure. All data were normalized to baseline values and reported as fold change from baseline.

### 2.4. Injection of neural inhibitors

Lidocaine HCl monohydrate (2.5 mg/kg) (Cat.# J6303506, Thermo Scientific™, Waltham, MA) was injected subcutaneously around the tibia receiving loading five minutes prior to loading in 2–6 month old male CD-1 mice ($n = 7$ control, $n = 8$ treated) in order to effectively block nerve activity in the hindlimb (Yin et al., 2021). Atropine sulfate monohydrate (2 mg/kg) (Cat.# A0550, TCI America™, Portland, OR) (Ha et al., 2020) ($n = 8$ control, $n = 11$ treated), and propranolol HCl (10 mg/kg) (Cat.# H2664506, Thermo Scientific™, Waltham, MA) (Barazi et al., 2021) ($n = 7$ control, n = 8 treated) were administered by intraperitoneal (IP) injection in 2–6 month old male CD-1 mice ~10 min prior to loading in order to block parasympathetic muscarinic and sympathetic autonomic nervous system activity, respectively. All drugs were dissolved in phosphate buffered saline (PBS) for injection delivery. Control mice were injected with similar volumes of vehicle solution (PBS) prior to undergoing tibia mechanical loading.

### 2.5. Strain gauging

Experimental strains were obtained from isolated right limb tibias of 6 month old male CD-1 mice ($n = 3$). Muscle and soft tissues were removed from the tibia using micro-dissection tools and the bone surface was prepared with 320-grit sandpaper and cleaned with acetone using a cotton applicator. A strain gauge (EA-06-015DJ-120/LE Vishay Precision Group, Malvern, PA) was then attached to the mid shaft region of the medial surface of the tibia using adhesive and electrical wires were carefully soldered to the strain gauge and multimeter was used to check the resistance. These wires were then soldered to the wires coming from the StrainSmart Data Acquisition system (System 7000 Vishay Precision Group, Malvern, PA) for strain recording. The tibia sample was placed in the loading fixture and mechanical loading was applied at 3 N, 5 N, 7 N and 9 N of load (2 Hz, 15 cycles) and the resultant strains were recorded. Average peak strains were plotted for each loading force.

### 2.6. Statistical analysis

Statistical analysis was performed with GraphPad Prism V.10 (GraphPad, La Jolla, CA). Animal data was analyzed by group comparisons and assessed for normality using the Shapiro-Wilks test. Outliers in the data were identified using Grubb's test and marked as an X in graphs and were removed prior to performing statistical analyses. Comparisons in the changes of heart rate, HRV and ECG parameters over time during the acute bone loading experiments were made using a Mixed Model ANOVA with Bonferroni post hoc analysis. One-way ANOVA with Bonferroni multiple comparisons post hoc analysis was utilized to compare heart rate and HRV changes in response to the different magnitudes of load. For the neural inhibitor injection studies, a two-tailed *t*-test was used to compare the vehicle and inhibitor-injected groups. In all cases, $P < 0.05$ was established a priori as the threshold for significance. All data are presented as boxplots indicating median, interquartile range and maximal and minimal range without outliers.

## 3. Results

To investigate cardiac functional alterations during bone mechanical loading, lead II electrocardiograms (ECG) were recorded in anesthetized adult male and female TOPGAL mice before, during, and after a two-and-a-half minute cyclical compressive loading protocol in the tibia of a single hindlimb (Fig. 1A). TOPGAL mice express a beta-galactosidase reporter system for Wnt signaling in bone and were utilized for these experiments in order to maintain consistency with previous bone loading studies performed by our group (Lara-Castillo et al., 2015; Lara-Castillo et al., 2023). Resting heart rates of anesthetized mice varied from ~430 to 625 beats per minute at baseline before the loading protocol. Control animals, which were placed into the loading apparatus but received no mechanical loading, showed no significant change in heart rate during the entirety of the experiment. Conversely, within seconds after initiation of compressive loading in the tibia at 9 N, we observed a significant immediate and transient decrease in heart rate (beats per minute, bpm), followed by its restoration to approximately baseline levels near the end of the two and a half minute loading period (Fig. 1B, Supplemental Table 1). This loading-dependent decrease in heart rate was observed in both male mice (control: 0.98 ± 0.02 vs. loaded: 0.94 ± 0.01 fold change from baseline; $p < 0.01$) and female mice (control: 0.99 ± 0.02 vs. loaded: 0.94 ± 0.01 fold change from baseline; $p < 0.01$) (Fig. 1C, Supplemental Table 1) and followed a similar temporal pattern in both sexes (Fig. 1C, Supplemental Table 1). RR interval was also significantly elevated during the loading period, indicating lowered heart rate in both male mice (control: 1.01 ± 0.005 vs. loaded: 1.05 ± 0.04 fold change from baseline; $p = 0.024$, data not shown) and female mice (control: 1.01 ± 0.008 vs. loaded: 1.05 ± 0.05 fold change from baseline; $p = 0.031$, data not shown). Concomitant to the reduction in heart rate with loading, the standard deviation of the RR interval (SDRR), a measure of overall heart rate variability (HRV), was significantly enhanced during loading in both male mice (control: 1.01 ± 0.04 vs. loaded: 1.24 ± 0.01 fold change from baseline; $p < 0.01$) and female mice (control: 1.02 ± 0.02 vs. loaded: 1.23 ± 0.08 fold change from baseline; $p < 0.01$) (Fig. 1D, Supplemental Table 1). Apart from the initial heart rate and HRV changes during loading, we did not find any sustained changes in heart rate or HRV relative to baseline during a 15-minute rest period subsequent to the end of loading (Fig. 1C-D, Supplemental Table 1).

Raw ECG signals were also examined during the loading experiments for characterization of cardiac depolarization and repolarization properties. In contrast to alterations in heart rate and HRV, we did not find any significant changes to atrial or ventricular conduction parameters, including PR interval, QRS interval, or QTc interval during tibia loading or during the subsequent 15 min, which suggests no effect of bone loading on atrioventricular coupling, ventricular depolarization, or ventricular repolarization, respectively (Fig. 2, Supplemental Table 1).

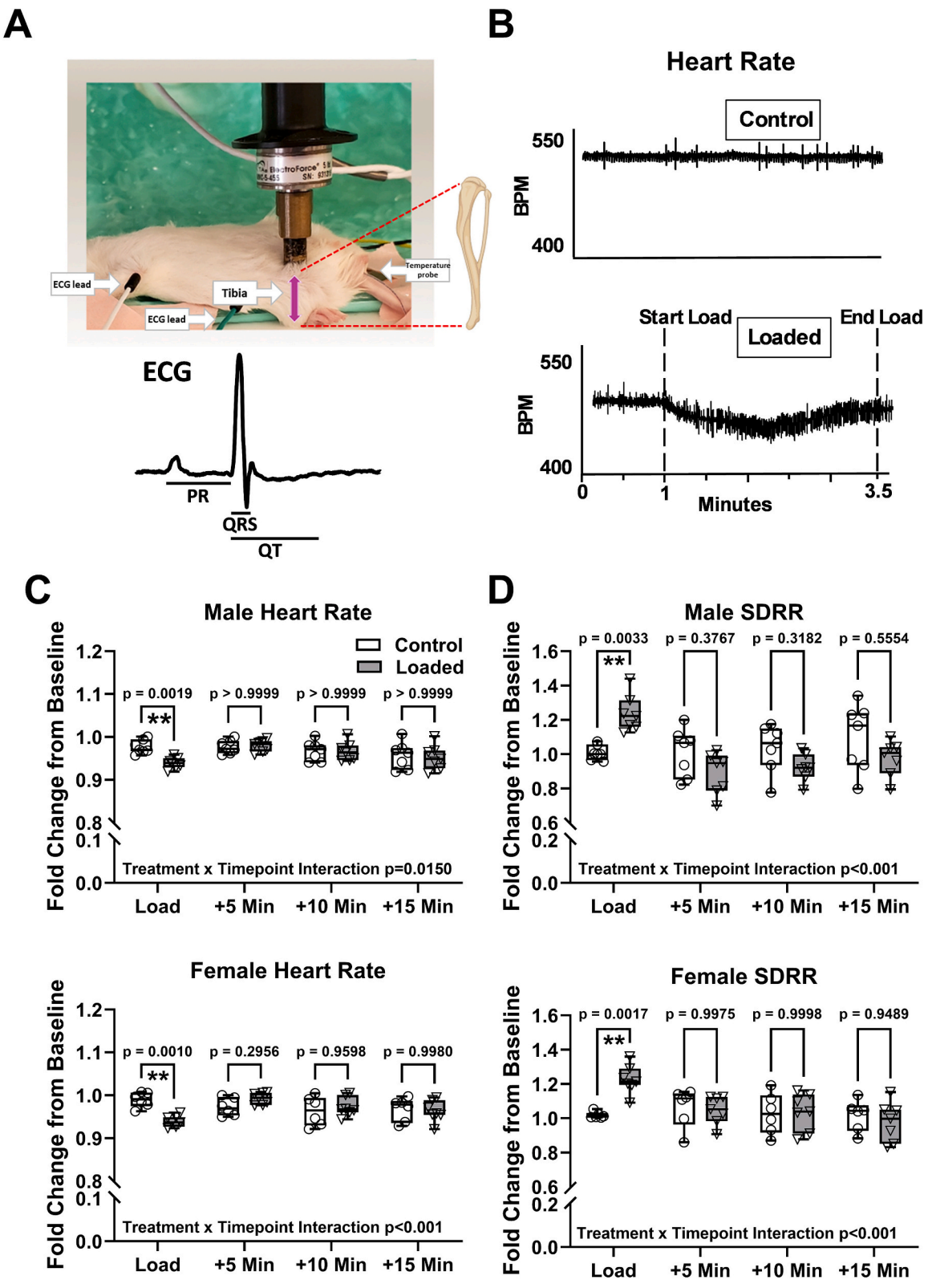


**Fig. 1. Heart rate and HRV during and after bone loading in adult mice.**
A) (Top) Photograph of the in vivo bone loading setup showing animal positioning, direction of loading of the tibia and placement of ECG and body temperature recording leads. (Bottom) Representative ECG signal from an adult mouse showing interval measurements. B) Tachograms of resting heart rate derived from ECG signals in anesthetized 5–6 month old control mice and in mice during the tibia mechanical loading protocol. C) Average male resting heart rate and standard deviation of the RR interval (SDRR) relative to baseline during mechanical loading and during 15 min after loading in 5–6 month old mice. D) Average female resting heart rate and standard deviation of the RR interval (SDRR) relative to baseline during mechanical loading and during 15 min after loading in 5–6 month old mice. $^{**}p < 0.01$ vs. control, Mixed Model ANOVA with Bonferroni post hoc analysis, $n = 6$–7 mice per group.

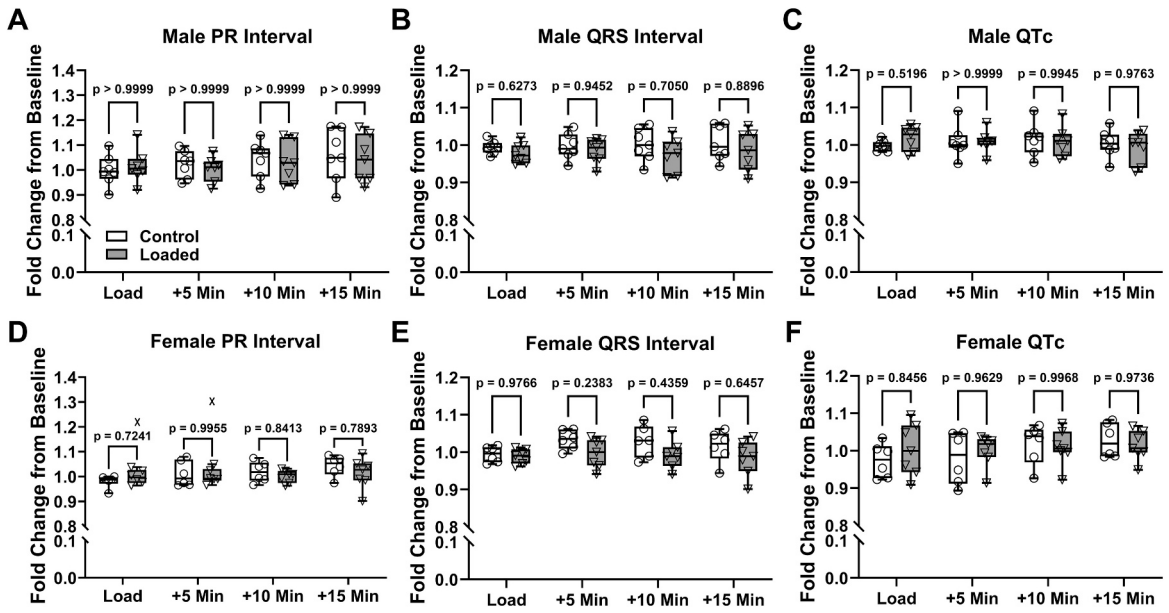


**Fig. 2. ECG intervals during and after bone loading in adult mice.**
Male PR interval (A), QRS interval (B), and corrected QT interval (QTc) (C) relative to baseline during mechanical loading and during 15 min after loading in 5–6 month old mice. Female PR interval (D), QRS interval (E), and corrected QT interval (QTc) (F) relative to baseline during mechanical loading and during 15 min after loading in 5–6 month old mice. Outlier data points are denoted as an X. Mixed Model ANOVA with Bonferroni post hoc analysis, n = 6–7 mice per group.

Given that bone experiences a variety of loading forces and strains that are dependent upon the type of physical activity, we next characterized the responsiveness of the heart in adult male CD-1 mice to physiological loads ranging from 1 N to 9 N. These loading parameters cover a range of physiologically relevant strain inputs and the use of wild-type CD-1 mice serves to determine the reproducibility of this reflex in non-transgenic mice. We utilized male mice for these follow up studies since cardiac responses to bone loading were similar among males and females. We found that loading of the tibia with 1 N or 2 N did not produce a significant change in heart rate (bpm) and HRV, while loading at 3 N and above activated a significant decrease in heart rate (Fig. 3A, Supplemental Table 2). Interestingly, compared to heart rate in control mice (0.99 ± 0.01 fold change from baseline) the relative reductions in heart rate were similar at 3 N (0.92 ± 0.08 fold change from baseline; $p < 0.05$ vs control) and 9 N (0.93 ± 0.06 fold change from baseline; $p < 0.05$ vs control) suggesting that a specific threshold level of strain must be attained in the tibia to activate these changes in heart rate. In line with these results, RR interval was also found to be significantly increased with loading at 3 N (1.10 ± 0.10 fold change from baseline; $p = 0.002$, data not shown) and 9 N (1.08 ± 0.08 fold change from baseline; $p = 0.027$, data not shown) compared to control (1.01 ± 0.006 fold change from baseline, data not shown). Additionally, HRV became elevated during loading with 3 N (1.38 ± 0.83 fold change from baseline; $p > 0.05$ vs control) and 9 N (1.66 ± 0.64 fold change from baseline; $p < 0.05$ vs control) compared to control mice (0.95 ± 0.20 fold change from baseline), although this parameter was only statistically significant for the 9 N load (Fig. 3B, Supplemental Table 2). To determine the levels of strain induced in the tibia by loading, strain gauge measurements were captured in isolated tibiae from CD-1 adult mice and showed that the loading magnitudes of 3 N - 9 N corresponds with an average strain of 370 με - 1307 με, respectively (Fig. 3C).

Considering the important impact of aging on many physiological and pathological processes, we performed further loading experiments on middle-aged mice (11–12 months old). Intriguingly, loading of the tibia in this older age group did not result in significant changes to heart rate (bpm) at either 3 N (control: 0.99 ± 0.005 vs. loaded: 0.99 ± 0.003 fold change from baseline; $p > 0.05$) (Fig. 4B, Supplemental Table 3) or at 9 N (control: 0.99 ± 0.007 vs. loaded: 0.98 ± 0.014 fold change from baseline; $p > 0.05$) (Fig. 4D, Supplemental Table 3) compared to control. When heart rate was analyzed as RR interval, there were also no significant differences when loading at 3 N (control: 1.00 ± 0.005 vs. loaded: 1.01 ± 0.003 fold change from baseline; $p = 0.935$, data not shown) and 9 N (control: 1.01 ± 0.007 vs. loaded: 1.02 ± 0.014 fold change from baseline; $p = 0.350$, data not shown). Similarly, HRV was not significantly altered during loading at either 3 N (control: 0.99 ± 0.12 vs. loaded: 0.99 ± 0.088 fold change from baseline; $p > 0.05$) (Fig. 4C, Supplemental Table 3) and at 9 N (control: 1.00 ± 0.24 vs. loaded: 1.19 ± 0.32 fold change from baseline; $p > 0.05$) (Fig. 4E, Supplemental Table 3) compared to control mice, although there was an observable non-significant increase in the average HRV during loading at 9 N. These data suggest that the responses of heart rate and HRV to mechanical loading may weaken with age. Next, average resting heart rate (adult: 530.9 ± 57.9 vs. middle age: 522.0 ± 50.8 bpm, Fig. 4F) and RR interval (adult: $n = 27$, 0.115 ± 0.014 vs. middle age: $n = 26$, 0.116 ± 0.012 s; $p = 0.661$, data not shown) were not different when comparing adult mice to middle age mice but average resting HRV was significantly reduced in the older animals (adult: 1.46 ± 0.72 vs. middle age: 1.04 ± 0.43 SDRR, Fig. 4G) indicating possible reduced autonomic control in this age group. Lastly, as was the case in the younger mice, loading at 3 N and 9 N in the middle-aged mice also did not produce significant changes to any of the ECG intervals (PR, QRS, QTc) (Fig. 5, Supplemental Table 3).

The changes in heart rate in response to bone mechanical loading were rapid, occurring within several seconds of initiation of bone loading and suggested that this physiological phenomenon was possibly mediated by a neuronal mechanism. We therefore investigated the involvement of nerves within the hindlimb and the autonomic nervous system through specific pharmacological blockade. First, to address activation of afferent neural components in the loaded hindlimb, we injected a voltage gated sodium channel blocker, lidocaine, into the area surrounding the tibia prior to the mechanical loading protocol while measuring ECG in anesthetized mice. The injection of lidocaine did not alter the resting heart rate on its own prior to bone-loading (Supplemental Fig. 1). Lidocaine pre-treated mice displayed a significant inhibition of the heart rate (bpm) decrease during bone loading compared to loaded mice treated with saline, suggesting that a neural afferent

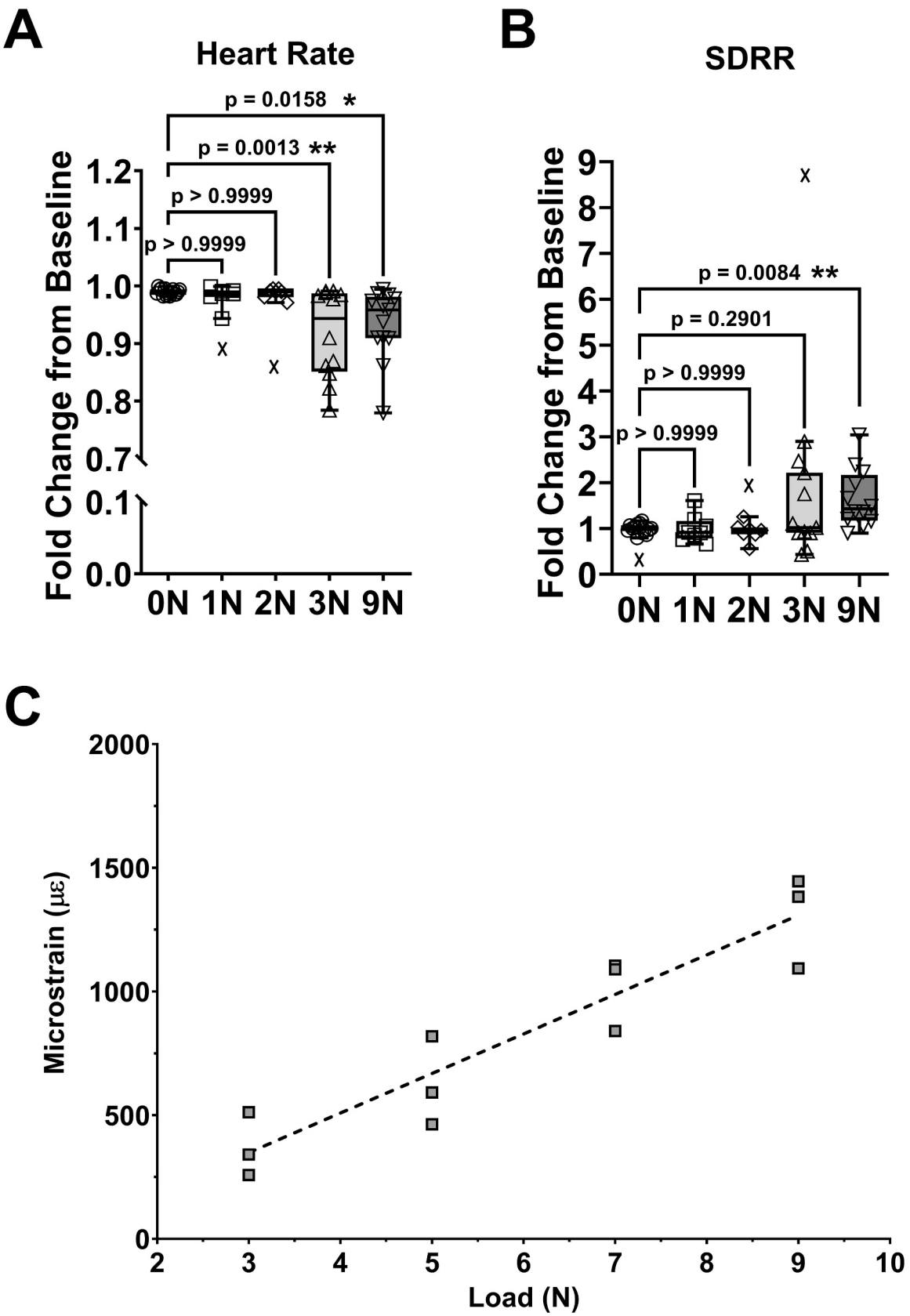


**Fig. 3. Effect of various magnitudes of bone load on heart rate and bone strain in adult mice.**
Average change in heart rate (A) and standard deviation of the RR interval (SDRR) (B) in response to tibia mechanical loading at 1–9 N in 2–6 month old male mice. Outlier data points are denoted as an X. **p $<$ 0.01, *$p$ $<$ 0.05, one-way ANOVA with Bonferroni post hoc analysis, $n$ = 7–13 mice per group. C) Strain gauge measurements in isolated tibia from adult 6 month old mice during mechanical loading at 3–9 N. Fitted line determined by simple linear regression, $n$ = 3 mice.

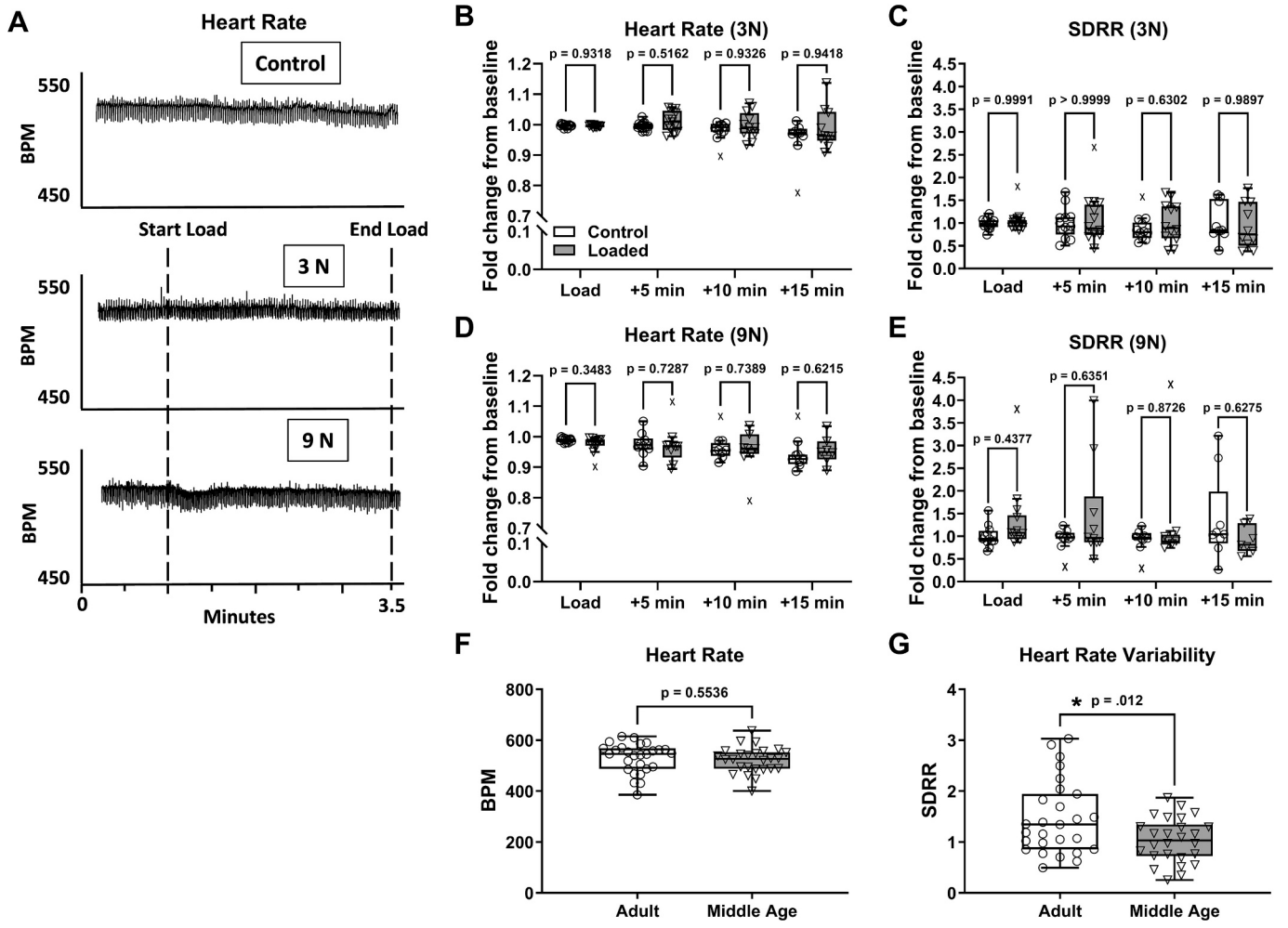


**Fig. 4. Heart rate and HRV during and after bone loading in middle-age mice.**
A) Tachograms of resting heart rate derived from ECG signals in 11–12 month old, anesthetized control mice and in mice during the tibia mechanical loading protocol at 3 N and 9 N. B) Average male resting heart rate and C) standard deviation of the RR interval (SDRR) relative to baseline during mechanical loading at 3 N and during 15 min after loading in 11–12 month old mice. D) Average male resting heart rate and E) standard deviation of the RR interval (SDRR) relative to baseline during mechanical loading at 9 N and during 15 min after loading in 11–12 month old mice. Mixed Model ANOVA with Bonferroni post hoc analysis, $n = 7$–13 mice per group. F) Average resting heart rate as beats per minute (BPM) and (G) heart rate variability as SDRR in adult and middle age male mice during anesthetized ECG. *$p < 0.05$, two-tailed $t$-test, $n = 26$–27 mice per group. Outlier data points are denoted as an X.

pathway mediates the signaling of bone loading to the heart (Fig. 6A, Supplemental Table 4). These results with lidocaine were similar when examining RR interval (Fig. 6A, Supplemental Table 4). Next, we determined if the autonomic nervous system was involved in this mechanism affecting heart rate by utilizing the inhibitor of parasympathetic muscarinic neurons, atropine, as well as sympathetic B1/B2 receptor blocker, propranolol, for pre-treatment in mice by IP injections prior to bone loading. Atropine pre-treatment did not result in a significant blockade of the heart rate (bpm) change in response to loading (Fig. 6B, Supplemental Table 4) or the RR interval (Fig. 6B, Supplemental Table 4). On the other hand, pre-treatment of propranolol effectively and significantly inhibited the heart rate (bpm) decrease during bone mechanical loading (Fig. 6C, Supplemental Table 4). RR interval showed similar results for the propranolol studies (Fig. 6C, Supplemental Table 4). These findings point towards reduced sympathetic tone as a major downstream mediator of heart rate reduction with bone loading in the efferent pathway of this bone-neuro-heart reflex.

## 4. Discussion

Bone exists in a dynamic interplay with external forces and other organ systems to maintain its homeostatic state within the body. In addition to its elegant self-regulatory ability, bone has emerged as a multifaceted organ, exhibiting endocrine functions (Robling and Bonewald, 2020) as well as being linked to the central/peripheral nervous system (Tomlinson et al., 2017; Chen et al., 2019). It is through these actions that bone exerts its modulatory ability on a number of tissues and itself (Karsenty and Olson, 2016). However, a connection with the heart, especially from the perspective of mechanical loading independent of other components of physical activity, has largely been unexplored. Here we describe a novel bone-neuro-heart reflex mediated by bone mechanical loading that becomes downregulated with aging. We show that a rapid and transient lowering of resting heart rate and enhancement of HRV occurred during a cyclic compressive loading protocol in a single tibia in adult anesthetized mice regardless of sex, but not in middle-aged mice. Parameters of intrinsic cardiac muscle conduction such as PR, QRS, and QTc remained unaffected with bone loading, suggesting this effect was mediated, likely, via changes in autonomic nervous system tone on the sinoatrial (SA) node and not a direct action on cardiac muscle or other cardiac conduction pathways. Inhibition of this bone-neuro-heart reflex with localized lidocaine suggested the mechanism was of neural origin, specifically via afferent nerves in the hindlimb. The use of propranolol demonstrated the potential involvement of receptors associated with the sympathetic

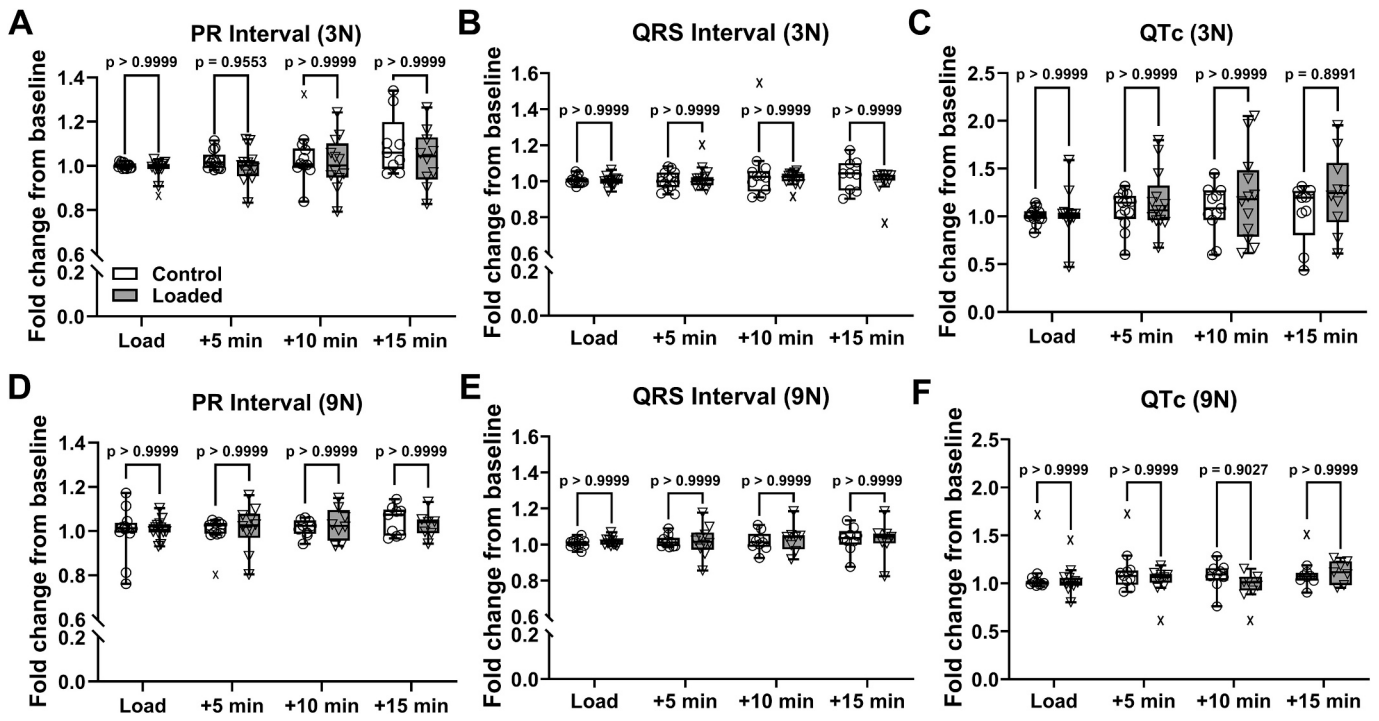


**Fig. 5. ECG intervals during and after bone loading in middle-age mice.**
Male PR interval (A), QRS interval (B), and corrected QT interval (QTc) (C) relative to baseline during mechanical loading and during 15 min after loading in 11–12 month old mice. Female PR interval (D), QRS interval (E), and corrected QT interval (QTc) (F) relative to baseline during mechanical loading and during 15 min after loading in 11–12 month old mice. Outlier data points are denoted as an X. Mixed Model ANOVA with Bonferroni post hoc analysis, n = 7–13 mice per group.

autonomic nervous system. The exact processing of this bone loading-mediated signal in the brain is still not completely resolved but may involve a neural relay mechanism within the hypothalamus as described previously (Gao et al., 2024), and/or direct signaling with autonomic control centers in the medulla to lower sympathetic tone on the heart (Gordan et al., 2015). These data highlight a novel connection between bone and the heart which may impact heart homeostasis and health during aging.

A consistent finding in the study involved the heart rate profile in response to tibial mechanical loading, which showed a transient decrease followed by recovery to near baseline levels by the end of the approximately two and a half minute loading protocol. The baroreflex produces one of the largest influences on the autonomic regulation of cardiac function and is indirectly coupled to changes in cardiac output via blood pressure in the aorta and carotid arteries (Kaufmann et al., 2020). Baroreceptors embedded within the aortic arch and carotid sinus respond to changes in stretch/blood pressure through compensatory activation of autonomic nuclei in the medulla to lower heart rate in cases of increased stretch/blood pressure and to raise heart rate when stretch/blood pressure becomes decreased (Kaufmann et al., 2020). Therefore, the acute decrease in heart rate during tibial mechanical loading may activate the baroreflex to induce heart rate recovery and underlie the observed transient heart rate profile in response to bone loading. Additional exploration will be needed to determine if additional compensatory mechanisms of the nervous system may be involved to induce recovery of heart rate or why the response is transient in nature.

Studies in transgenic and genetic deletion mouse models have identified a central control mechanism governing skeletal bone mass homeostasis involving the central nervous system and the sympathetic and parasympathetic arms of the autonomic nervous system (Chen et al., 2019; Takeda et al., 2002; Shi et al., 2010). One molecular mediator involved in the regulation of bone mass by the central nervous system is the peptide neuromedin U, which has been demonstrated to be an important downstream mediator of SNS-based control of bone mass by leptin signaling (Sato et al., 2007). Interestingly, intracerebroventricular injection of neuromedin U dose-dependently increased resting heart rate and mean arterial blood pressure in rats (Chu et al., 2002). These findings may suggest an intersection of shared neural pathways or mechanisms regulating both bone mass accrual and cardiac function, which are in line with our findings showing a coupled responsiveness of heart rhythm properties with loading-induced strain in bone. However, whether this bone-neuro-heart connection plays a specific physiological role on the regulation of the heart or if it merely represents a generalized effect on autonomic tone to produce favorable conditions for the skeleton remains unclear.

We employed a physiological bone loading protocol under a range of loading forces correlating with normal daily activity and up to a high impact style of activity. Utilization of the 9 N loading protocol in the tibia produces sufficient microstrain to activate osteogenic signaling in bone cells and a bone anabolic response as previously reported by our group and others using this model (Robinson et al., 2006; Lara-Castillo et al., 2023). Through strain gauging studies we found that ex-vivo tibial bone loading in 6-month-old CD-1 mice ranging from 3 N to 9 N resulted in mean tibial microstrain ranging from 370.25 με to 1307.08 με, respectively. For reference in humans, a study focusing on the relationship between physical activity in humans and microstrain on the tibia observed that the mean tibial microstrain during walking at 6.1 km per hour was 658.11 με, reaching as high as 1011.15 με when the subjects were carrying an additional 35 kg of weight (Wang et al., 2019). Incredibly, tibial microstrain reached magnitudes of >2000 με in the middle of the tibia and >3000 με in the distal third of the tibia when human subjects landed from a 45-centimeter vertical jump, while running on the treadmill at 13 kilometers per hour produced a range from 101 to 1950 με (Milgrom et al., 2022). Other activities for which human tibial microstrain data have been reported include stepmaster (1006 με), bicycling (291 με), and leg press (883 με) (Milgrom et al., 2000). In addition to these data, we selected load forces of 1–9 N based on Harold Frost's "Mechanostat Theory," in which Frost details the

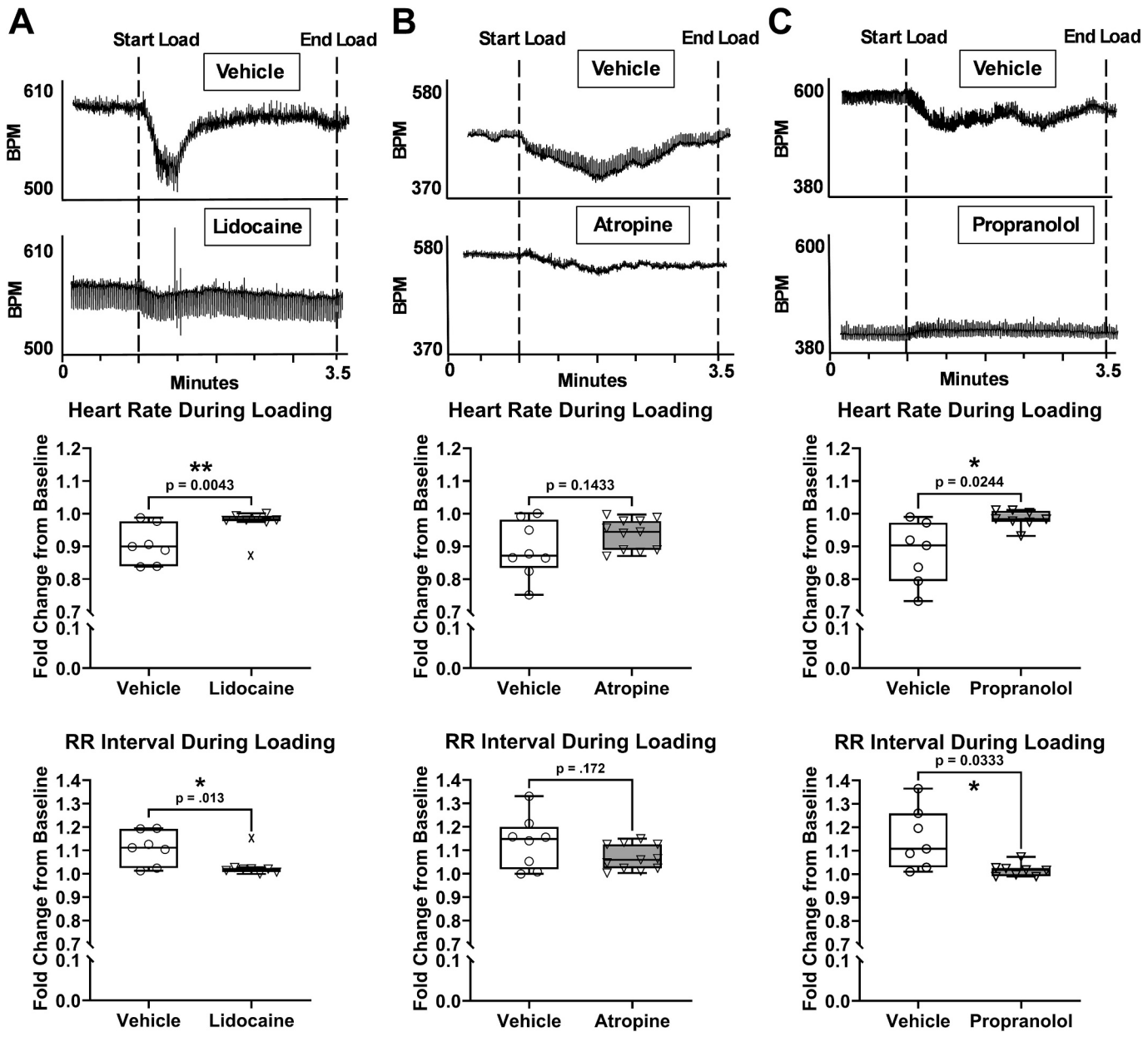


**Fig. 6. Effect of neural blockade on heart rate during bone loading in adult mice.**
Representative tachograms showing heart rate (Top), average changes in heart rate relative to baseline (Middle), and average changes to RR interval (Bottom) in response to mechanical loading in mice pre-treated with lidocaine injected in the hindlimb (A), atropine injected IP (B), and propranolol injected IP (C). Outlier data points are denoted as an X. $^{**}p < 0.01$, $^{*}p < 0.05$, two-tailed t-test, n = 7–11 mice per group.

evidence for various thresholds of bone loading. Loads of 300–1500 με result in bone maintenance due to physiologic loading while loads of >3000 με result in damage to the bone microarchitecture due to non-physiologic strain (Tyrovola, 2015). Our experiments maintain tibial microstrain in the physiologic loading range (300–1500 με) represent the effects of typical daily exertion on the tibia while avoiding levels of microstrain that have been shown to cause harm.

Our results suggest that the influence of bone loading on heart function is diminished by as early as middle age. A study measuring strain levels in the tibia during loading in CD-1 mice found that comparable, albeit slightly less, magnitudes of load were necessary in middle-aged mice to elicit similar amounts of strain at both low and high magnitudes of loading compared to young mice (Holguin et al., 2016). This supports other mechanisms, such as nervous system-based or cardiac changes, underlying these findings with early aging. In the setting of aging and age-related disorders like osteoporosis, bone shows alterations to the osteocyte-dendritic network, increased osteocyte apoptosis, reduced nerve density, and a decrease in the ability to respond to mechanical loading (Armas and Recker, 2012; Tomlinson et al., 2020). While reduced nerve fiber content has been documented within the bones of old animals compared to young animals (Tomlinson et al., 2020), little is known of the changes to nerves in bone occurring at middle age, which could help interpret our findings at this age. It is possible that the reduced cardiac responses to bone loading in mice at middle age may represent an early alteration in bone-neural pathways which could preface further aging-related bone loss or autonomic dysfunction. However, despite these findings, it remains unclear whether the reduced response of heart rate and HRV to bone loading are a cause or consequence of altered autonomic tone at middle age. Since the middle-aged mice in this study had evidence of altered autonomic control showing significantly lower baseline HRV compared to younger adult mice even before loading was performed, this may suggest that the

dysfunction may reside at the level of the cardiac environment and its ability to effectively respond to changes in autonomic neural impulses, instead of at the level of the bone. Indeed, human studies have shown alterations to autonomic influence on the heart in middle-aged individuals (Moodithaya and Avadhany, 2012). Additionally, circulating serum levels of norepinephrine gradually rise during the course of aging, which may lead to increased baseline cardiac adrenergic signaling and interference with the autonomic nervous system signals in response to bone loading in middle-aged mice (Kaplon et al., 2011). A better understanding of the nature of bone-neuro-heart crosstalk pathways could provide insight into the clinical connections of bone and cardiac health and may lead to development of new and superior treatment strategies for the presently undertreated and widespread diseases of osteoporosis and cardiovascular dysfunction.

There are several limitations which should be considered when interpreting the results of this study. In order to maintain a controlled loading environment without the influence of skeletal muscle contraction, we performed bone mechanical loading on mice under isoflurane anesthesia, which is known to depress autonomic nervous control (Campagna et al., 2003). Therefore, it is possible that nerve responses and signaling may differ in conscious animals or in middle-age mice compared to young mice leading to the observed age-dependent results. Next, we did not simultaneously measure changes in blood pressure or cardiac filling to avoid a disturbing our protocol and to control physiological variables that these procedures may introduce. While we have documented this association of bone loading and heart rate, the response may involve additional physiological components. The neuronal inhibitors used in this study can also have systemic effects including in bone (Kim et al., 2023; Liu et al., 2011; Wu et al., 2021), and on vascular smooth muscle tone and blood pressure (Ketabi et al., 2012; Merrick and Holcslaw, 1981; Priviero et al., 2006), which may have also contributed to changes in cardiac function. Additionally, propranolol effectively lowered the resting heart rate of the animals in this study and this confounding effect should be considered in the interpretation of the mechanistic results. We employed a mechanical loading protocol we have previously shown to activate anabolic signaling in the tibia and ulna of mice. It remains unknown if loading of different bone types produces similar responses in the heart. Lastly, the impact of different loading protocol variables such as frequency, rest period, and dwell time on the bone-neuro-heart response was not addressed in this study. In conclusion, our findings that bone loading in the tibia modulates heart rate and HRV in an age-dependent manner support the idea of the skeletal and cardiovascular systems as tightly intertwined entities in physiology, health, and aging.

Supplementary data to this article can be found online at https://doi.org/10.1016/j.bonr.2025.101844.

## CRediT authorship contribution statement

**Julian A. Vallejo:** Conceptualization, Data curation, Formal analysis, Funding acquisition, Investigation, Methodology, Validation, Visualization, Writing – original draft. **Mark Gray:** Data curation, Formal analysis, Investigation, Visualization, Writing – review & editing. **Jackson Klump:** Formal analysis, Investigation, Writing – review & editing. **Andrew Wacker:** Formal analysis, Investigation, Writing – review & editing. **Mark Dallas:** Formal analysis, Investigation, Writing – review & editing. **Mark L. Johnson:** Funding acquisition, Methodology, Project administration, Resources, Supervision, Writing – review & editing. **Michael J. Wacker:** Conceptualization, Funding acquisition, Methodology, Project administration, Supervision, Writing – review & editing.

## Funding

This student/project was supported by the Health Resources and Services Administration (HRSA) of the U.S. Department of Health and Human Services (HHS) Grant T99HP39202 (MJW) as part of an award totaling $18,000,000 with 10 % financed with non-governmental sources. The contents are those of the author(s) and do not necessarily represent the official views of, nor an endorsement, by HRSA, HHS, or the U.S. Government. For more information, please visit HRSA.gov. This project was also supported by NIH-NIA Program Project Grant P01AG039355 (MJW, MLJ) and NIH-NIA Diversity Supplement P01AG039355-08 (JAV).

## Declaration of competing interest

The authors of this study have no conflicts of interest to disclose.

## Acknowledgements

We would like to thank Ms. Makayla Ayres for technical assistance with experiments and Dr. Thiagarajan Ganesh for advice related to data interpretation. The graphical abstract was created in BioRender. Vallejo, J. (2024) https://BioRender.com/y27e981.

## Data availability

Data will be made available on request.

## References

Armas, L.A., Recker, R.R., 2012. Pathophysiology of osteoporosis: new mechanistic insights. Endocrinol. Metab. Clin. N. Am. 41 (3), 475–486.
Bansilal, S., Castellano, J.M., Fuster, V., 2015. Global burden of CVD: focus on secondary prevention of cardiovascular disease. Int. J. Cardiol. 201 (Suppl. 1), S1–S7.
Barazi, N., Polidovitch, N., Debi, R., Yakobov, S., Lakin, R., Backx, P.H., 2021. Dissecting the roles of the autonomic nervous system and physical activity on circadian heart rate fluctuations in mice. Front. Physiol. 12, 692247.
Berger, J.M., Singh, P., Khrimian, L., Morgan, D.A., Chowdhury, S., Arteaga-Solis, E., Horvath, T.L., Domingos, A.I., Marsland, A.L., Yadav, V.K., Rahmouni, K., Gao, X.B., Karsenty, G., 2019. Mediation of the acute stress response by the skeleton. Cell Metab. 30 (5), 890–902.e8.
Böhm, M., Reil, J.C., Deedwania, P., Kim, J.B., Borer, J.S., 2015. Resting heart rate: risk indicator and emerging risk factor in cardiovascular disease. Am. J. Med. 128 (3), 219–228.
Bonewald, L.F., Johnson, M.L., 2008. Osteocytes, mechanosensing and Wnt signaling. Bone 42 (4), 606–615.
Bonewald, L.F., Wacker, M.J., 2013. FGF23 production by osteocytes. Pediatr. Nephrol. 28 (4), 563–568.
Campagna, J.A., Miller, K.W., Forman, S.A., 2003. Mechanisms of actions of inhaled anesthetics. N. Engl. J. Med. 348 (21), 2110–2124.
Chen, H., Hu, B., Lv, X., Zhu, S., Zhen, G., Wan, M., Jain, A., Gao, B., Chai, Y., Yang, M., Wang, X., Deng, R., Wang, L., Cao, Y., Ni, S., Liu, S., Yuan, W., Chen, H., Dong, X., Guan, Y., Yang, H., Cao, X., 2019. Prostaglandin E2 mediates sensory nerve regulation of bone homeostasis. Nat. Commun. 10 (1), 181.
Cherian, P.P., Siller-Jackson, A.J., Gu, S., Wang, X., Bonewald, L.F., Sprague, E., Jiang, J. X., 2005. Mechanical strain opens connexin 43 hemichannels in osteocytes: a novel mechanism for the release of prostaglandin. Mol. Biol. Cell 16 (7), 3100–3106.
Chu, C., Jin, Q., Kunitake, T., Kato, K., Nabekura, T., Nakazato, M., Kangawa, K., Kannan, H., 2002. Cardiovascular actions of central neuromedin U in conscious rats. Regul. Pept. 105 (1), 29–34.
Dallas, S.L., Prideaux, M., Bonewald, L.F., 2013. The osteocyte: an endocrine cell ... And more. Endocr. Rev. 34 (5), 658–690.
Elefteriou, F., 2018. Impact of the autonomic nervous system on the skeleton. Physiol. Rev. 98 (3), 1083–1112.
Fang, S.C., Wu, Y.L., Tsai, P.S., 2020. Heart rate variability and risk of all-cause death and cardiovascular events in patients with cardiovascular disease: a meta-analysis of cohort studies. Biol. Res. Nurs. 22 (1), 45–56.
Ferron, M., McKee, M.D., Levine, R.L., Ducy, P., Karsenty, G., 2012. Intermittent injections of osteocalcin improve glucose metabolism and prevent type 2 diabetes in mice. Bone 50 (2), 568–575.
Gao, F., Hu, Q., Chen, W., Li, J., Qi, C., Yan, Y., Qian, C., Wan, M., Ficke, J., Zheng, J., Cao, X., 2024. Brain regulates weight bearing bone through PGE2 skeletal interoception: implication of ankle osteoarthritis and pain. Bone Res. 12 (1), 16.
Gordan, R., Gwathmey, J.K., Xie, L.H., 2015. Autonomic and endocrine control of cardiovascular function. World J. Cardiol. 7 (4), 204–214.
Graves, J.M., Vallejo, J.A., Hamill, C.S., Wang, D., Ahuja, R., Patel, S., Faul, C., Wacker, M.J., 2021. Fibroblast growth factor 23 (FGF23) induces ventricular arrhythmias and prolongs QTc interval in mice in an FGF receptor 4-dependent manner. Am. J. Physiol. Heart Circ. Physiol. 320 (6), H2283–H2294.
Ha, T.W., Oh, B., Kang, J.O., 2020. Electrocardiogram recordings in anesthetized mice using Lead II. J. Vis. Exp. 160.

Holguin, N., Brodt, M.D., Silva, M.J., 2016. Activation of Wnt signaling by mechanical loading is impaired in the bone of old mice. J. Bone Miner. Res. 31 (12), 2215–2226.
Huang, J., Romero-Suarez, S., Lara, N., Mo, C., Kaja, S., Brotto, L., Dallas, S.L., Johnson, M.L., Jähn, K., Bonewald, L.F., Brotto, M., 2017. Crosstalk between MLO-Y4 osteocytes and C2C12 muscle cells is mediated by the Wnt/β-catenin pathway. JBMR Plus 1 (2), 86–100.
Jung, M.H., Youn, H.J., Ihm, S.H., Jung, H.O., Hong, K.S., 2018. Heart rate and bone mineral density in older women with hypertension: results from the Korea National Health and Nutritional Examination Survey. J. Am. Geriatr. Soc. 66 (6), 1144–1150.
Kamel, M.A., Picconi, J.L., Lara-Castillo, N., Johnson, M.L., 2010. Activation of β-catenin signaling in MLO-Y4 osteocytic cells versus 2T3 osteoblastic cells by fluid flow shear stress and PGE2: implications for the study of mechanosensation in bone. Bone 47 (5), 872–881.
Kaplon, R.E., Walker, A.E., Seals, D.R., 2011. Plasma norepinephrine is an independent predictor of vascular endothelial function with aging in healthy women. J. Appl. Physiol. (1985) 111 (5), 1416–1421.
Karsenty, G., Olson, E.N., 2016. Bone and muscle endocrine functions: unexpected paradigms of inter-organ communication. Cell 164 (6), 1248–1256.
Kaufmann, H., Norcliffe-Kaufmann, L., Palma, J.A., 2020. Baroreflex dysfunction. N. Engl. J. Med. 382 (2), 163–178.
Ketabi, M., Shamami, M.S., Alaie, M., Shamami, M.S., 2012. Influence of local anesthetics with or without epinephrine 1/80000 on blood pressure and heart rate: a randomized double-blind experimental clinical trial. Dent. Res. J. (Isfahan) 9 (4), 437–440.
Kim, E.J., Yoon, J.U., Kim, C.H., Yoon, J.Y., Kim, J.Y., Kim, H.S., Choi, E.J., 2023. Lidocaine inhibits osteogenic differentiation of human dental pulp stem cells in vitro. J. Int. Med. Res. 51 (2), 3000605231152100.
Kola, S.K., Begonia, M.T., Tiede-Lewis, L.M., Laughrey, L.E., Dallas, S.L., Johnson, M.L., Ganesh, T., 2020. Osteocyte lacunar strain determination using multiscale finite element analysis. Bone Rep. 12, 100277.
Lara-Castillo, N., Kim-Weroha, N.A., Kamel, M.A., Javaheri, B., Ellies, D.L., Krumlauf, R. E., Thiagarajan, G., Johnson, M.L., 2015. In vivo mechanical loading rapidly activates β-catenin signaling in osteocytes through a prostaglandin mediated mechanism. Bone 76, 58–66.
Lara-Castillo, N., Masunaga, J., Brotto, L., Vallejo, J.A., Javid, K., Wacker, M.J., Brotto, M., Bonewald, L.F., Johnson, M.L., 2023. Muscle secreted factors enhance activation of the PI3K/Akt and β-catenin pathways in murine osteocytes. Bone 174, 116833.
Lary, C.W., Hinton, A.C., Nevola, K.T., Shireman, T.I., Motyl, K.J., Houseknecht, K.L., Lucas, F.L., Hallen, S., Zullo, A.R., Berry, S.D., Kiel, D.P., 2020. Association of beta blocker use with bone mineral density in the Framingham osteoporosis study: a cross-sectional study. JBMR Plus 4 (9), e10388.
Li, X., Zhang, Y., Kang, H., Liu, W., Liu, P., Zhang, J., Harris, S.E., Wu, D., 2005. Sclerostin binds to LRP5/6 and antagonizes canonical Wnt signaling. J. Biol. Chem. 280 (20), 19883–19887.
Li, Z., Meyers, C.A., Chang, L., Lee, S., Li, Z., Tomlinson, R., Hoke, A., Clemens, T.L., James, A.W., 2019. Fracture repair requires TrkA signaling by skeletal sensory nerves. J. Clin. Invest. 129 (12), 5137–5150.
Liu, P.S., Chen, Y.Y., Feng, C.K., Lin, Y.H., Yu, T.C., 2011. Muscarinic acetylcholine receptors present in human osteoblast and bone tissue. Eur. J. Pharmacol. 650 (1), 34–40.
Marcovitz, P.A., Tran, H.H., Franklin, B.A., O'Neill, W.W., Yerkey, M., Boura, J., Kleerekoper, M., Dickinson, C.Z., 2005. Usefulness of bone mineral density to predict significant coronary artery disease. Am. J. Cardiol. 96 (8), 1059–1063.
Mera, P., Laue, K., Ferron, M., Confavreux, C., Wei, J., Galán-Díez, M., Lacampagne, A., Mitchell, S.J., Mattison, J.A., Chen, Y., Bacchetta, J., Szulc, P., Kitsis, R.N., de Cabo, R., Friedman, R.A., Torsitano, C., McGraw, T.E., Puchowicz, M., Kurland, I., Karsenty, G., 2016. Osteocalcin signaling in Myofibers is necessary and sufficient for optimum adaptation to exercise. Cell Metab. 23 (6), 1078–1092.
Merrick, B.A., Holcslaw, T.L., 1981. Direct vasodilator activity of atropine in the rat perfused hindlimb preparation. Clin. Exp. Pharmacol. Physiol. 8 (3), 277–281.
Milgrom, C., Finestone, A., Simkin, A., Ekenman, I., Mendelson, S., Millgram, M., Nyska, M., Larsson, E., Burr, D., 2000. In-vivo strain measurements to evaluate the strengthening potential of exercises on the tibial bone. J. Bone Joint Surg. (Br.) 82 (4), 591–594.
Milgrom, C., Voloshin, A., Novack, L., Milgrom, Y., Ekenman, I., Finestone, A.S., 2022. In vivo strains at the middle and distal thirds of the tibia during exertional activities. Bone Rep. 16, 101170.
Mo, C., Romero-Suarez, S., Bonewald, L., Johnson, M., Brotto, M., 2012. Prostaglandin E2: from clinical applications to its potential role in bone- muscle crosstalk and myogenic differentiation. Recent Pat. Biotechnol. 6 (3), 223–229.
Mo, C., Zhao, R., Vallejo, J., Igwe, O., Bonewald, L., Wetmore, L., Brotto, M., 2015. Prostaglandin E2 promotes proliferation of skeletal muscle myoblasts via EP4 receptor activation. Cell Cycle 14 (10), 1507–1516.
Moodithaya, S., Avadhany, S.T., 2012. Gender differences in age-related changes in cardiac autonomic nervous function. J. Aging Res. 2012, 679345.
Nakashima, T., Hayashi, M., Fukunaga, T., Kurata, K., Oh-Hora, M., Feng, J.Q., Bonewald, L.F., Kodama, T., Wutz, A., Wagner, E.F., Penninger, J.M., Takayanagi, H., 2011. Evidence for osteocyte regulation of bone homeostasis through RANKL expression. Nat. Med. 17 (10), 1231–1234.
Norvell, S.M., Alvarez, M., Bidwell, J.P., Pavalko, F.M., 2004. Fluid shear stress induces beta-catenin signaling in osteoblasts. Calcif. Tissue Int. 75 (5), 396–404.
Priviero, F.B., Teixeira, C.E., Toque, H.A., Claudino, M.A., Webb, R.C., De Nucci, G., Zanesco, A., Antunes, E., 2006. Vasorelaxing effects of propranolol in rat aorta and mesenteric artery: a role for nitric oxide and calcium entry blockade. Clin. Exp. Pharmacol. Physiol. 33 (5–6), 448–455.
Robinson, J.A., Chatterjee-Kishore, M., Yaworsky, P.J., Cullen, D.M., Zhao, W., Li, C., Kharode, Y., Sauter, L., Babij, P., Brown, E.L., Hill, A.A., Akhter, M.P., Johnson, M.L., Recker, R.R., Komm, B.S., Bex, F.J., 2006. Wnt/beta-catenin signaling is a normal physiological response to mechanical loading in bone. J. Biol. Chem. 281 (42), 31720–31728.
Robling, A.G., Bonewald, L.F., 2020. The osteocyte: new insights. Annu. Rev. Physiol. 82, 485–506.
Rodríguez-Gómez, I., Gray, S.R., Ho, F.K., Petermann-Rocha, F., Welsh, P., Cleland, J., Iliodromiti, S., Ara, I., Pell, J., Sattar, N., Ferguson, L.D., Celis-Morales, C., 2022. Osteoporosis and its association with cardiovascular disease, respiratory disease, and cancer: findings from the UK biobank prospective cohort study. Mayo Clin. Proc. 97 (1), 110–121.
Sato, S., Hanada, R., Kimura, A., Abe, T., Matsumoto, T., Iwasaki, M., Inose, H., Ida, T., Mieda, M., Takeuchi, Y., Fukumoto, S., Fujita, T., Kato, S., Kangawa, K., Kojima, M., Shinomiya, K., Takeda, S., 2007. Central control of bone remodeling by neuromedin U. Nat. Med. 13 (10), 1234–1240.
Sayilekshmy, M., Hansen, R.B., Delaissé, J.M., Rolighed, L., Andersen, T.L., Heegaard, A. M., 2019. Innervation is higher above bone remodeling surfaces and in cortical pores in human bone: lessons from patients with primary hyperparathyroidism. Sci. Rep. 9 (1), 5361.
Shi, Y., Oury, F., Yadav, V.K., Wess, J., Liu, X.S., Guo, X.E., Murshed, M., Karsenty, G., 2010. Signaling through the M(3) muscarinic receptor favors bone mass accrual by decreasing sympathetic activity. Cell Metab. 11 (3), 231–238.
Takeda, S., Elefteriou, F., Levasseur, R., Liu, X., Zhao, L., Parker, K.L., Armstrong, D., Ducy, P., Karsenty, G., 2002. Leptin regulates bone formation via the sympathetic nervous system. Cell 111 (3), 305–317.
Tankó, L.B., Christiansen, C., Cox, D.A., Geiger, M.J., McNabb, M.A., Cummings, S.R., 2005. Relationship between osteoporosis and cardiovascular disease in postmenopausal women. J. Bone Miner. Res. 20 (11), 1912–1920.
Tatsumi, S., Ishii, K., Amizuka, N., Li, M., Kobayashi, T., Kohno, K., Ito, M., Takeshita, S., Ikeda, K., 2007. Targeted ablation of osteocytes induces osteoporosis with defective mechanotransduction. Cell Metab. 5 (6), 464–475.
Tomlinson, R.E., Li, Z., Li, Z., Minichiello, L., Riddle, R.C., Venkatesan, A., Clemens, T.L., 2017. NGF-TrkA signaling in sensory nerves is required for skeletal adaptation to mechanical loads in mice. Proc. Natl. Acad. Sci. USA 114 (18), E3632–e3641.
Tomlinson, R.E., Christiansen, B.A., Giannone, A.A., Genetos, D.C., 2020. The role of nerves in skeletal development, adaptation, and aging. Front. Endocrinol. (Lausanne) 11, 646.
Tosun, A., Doğru, M.T., Aydn, G., Keleş, I., Arslan, A., Güneri, M., Orkun, S., Ebinç, H., 2011. Does autonomic dysfunction exist in postmenopausal osteoporosis? Am. J. Phys. Med. Rehabil. 90 (12), 1012–1019.
Touchberry, C.D., Green, T.M., Tchikrizov, V., Mannix, J.E., Mao, T.F., Carney, B.W., Girgis, M., Vincent, R.J., Wetmore, L.A., Dawn, B., Bonewald, L.F., Stubbs, J.R., Wacker, M.J., 2013. FGF23 is a novel regulator of intracellular calcium and cardiac contractility in addition to cardiac hypertrophy. Am. J. Physiol. Endocrinol. Metab. 304 (8), E863–E873.
Tyrovola, J.B., 2015. The "Mechanostat theory" of frost and the OPG/RANKL/RANK system. J. Cell. Biochem. 116 (12), 2724–2729.
Wang, H., Kia, M., Dickin, D.C., 2019. Influences of load carriage and physical activity history on tibia bone strain. J. Sport Health Sci. 8 (5), 478–485.
Wu, Y., Zhang, Q., Zhao, B., Wang, X., 2021. Effect and mechanism of propranolol on promoting osteogenic differentiation and early implant osseointegration. Int. J. Mol. Med. 48 (4).
Yin, Q., Zhang, W., Ke, B., Liu, J., Zhang, W., 2021. Lido-OH, a hydroxyl derivative of lidocaine. produced a similar local anesthesia profile as lidocaine with reduced systemic toxicities, Front. Pharmacol. 12, 678437.